JOURNAL OF MATERIALS SCIENCE 30 (1995) 4801–4816

Chemical diffusion in non-stoichiometric metal sulphides

S. MROWEC
Department of Solid State Chemistry, University of Mining and Metallurgy, al. Mickiewicza 30, 30-059 Cracow, Poland

K. HASHIMOTO
Institute for Materials Research, Tohoku University, Sendai, 980-77, Japan

Transport properties of transition metal sulphides have been discussed in terms of chemical- and self-diffusion coefficients. It has been shown that in the case of highly non-stoichiometric sulphides ($Co_{1-y}S$) the chemical diffusion coefficient may easily be obtained from thermogravimetric measurements of re-equilibration kinetics. If the non-stoichiometry and thereby defect concentration is low ($Mn_{1-y}S$), the re-equilibration kinetics is difficult or impossible to follow thermogravimetrically, and the electrical conductivity method can be applied. If the non-stoichiometry of a given metal sulphide is known as a function of temperature and sulphur activity, chemical diffusion data may successfully be utilized for calculation of parabolic rate constants of metal sulphidation and to obtain better insight into the growth mechanism of the sulphide scale. Using this procedure it has been shown that the sulphide scales on cobalt and manganese grow by the outward volume diffusion of cations. The chemical diffusion coefficient may also be used in the calculation of the self-diffusion coefficient of cations (or anions) if the non-stoichiometry data of a given sulphide are available. It has been shown that the self-diffusion coefficients of manganese in $Mn_{1-y}S$ obtained in such a way are in full agreement with those determined experimentally.

1. Introduction

Transition metal sulphides show generally much higher deviation from stoichiometry and thereby higher defect concentrations than corresponding oxides [1–3] and this is considered to be the main reason for the rapid degradation of high-temperature alloys in sulphur-containing atmospheres [3–5]. However, the mechanism of sulphide corrosion is still not satisfactorily understood. Such a situation results mainly from much greater experimental difficulties in studying the defect and transport properties of sulphides than those of oxides. In fact, the only sulphide in which the self-diffusion rate of cations and anions has been systematically studied as a function of temperature and sulphur activity, is the non-stoichiometric ferrous sulphide, $Fe_{1-y}S$ [6]. As a consequence, the mechanism of iron sulphidation could be explained in detail [7–9]. It has been shown that the sulphide scale on iron grows by the outward volume diffusion of cations at surprisingly low temperatures ($> 400\,^{\circ}C$). These results are in dramatic contrast with those obtained in the case of metal oxidation in which the grain-boundary diffusion participates in the overall matter transport through oxide scales up to much higher temperatures ([4], p. 206, [10]). For instance, in the case of nickel oxidation, the outward diffusion of cations proceeds mainly along the grain boundaries of NiO-scale up to about $900\,^{\circ}C$ ([4] p. 206, [10–12]), and Cr_2O_3 scale on chromium is believed to grow virtually only as a result of the grain-boundary diffusion of cations at temperatures exceeding $1000\,^{\circ}C$.

It should be stressed, however, that transition metal sulphides are less thermodynamically stable and consequently generally melt at lower temperatures than the corresponding oxides [1–3]. Thus, Tammann's temperature for sulphides, that is, the temperature where the transition from grain-boundary diffusion to volume diffusion occurs, is generally lower than those for oxides. This fact strongly suggests that volume diffusion may prevail in the matter transport through the sulphide scales at relatively low temperatures, as in the case of iron sulphidation. To verify this conclusion and thereby to obtain more insight into the mechanism of sulphide corrosion, more information on transport properties of sulphides is urgently needed.

The aim of the present work was to show that rather simple chemical diffusion measurements may successfully be utilized for indirect evaluation of defect mobility and self-diffusion coefficients in non-stoichiometric sulphides, two important quantities, the direct determination of which is very difficult for sulphides. Three selected examples will be discussed. The first,

0022–2461

metal-deficient cobaltous sulphide, $Co_{1-y}S$, represents the majority of transition metal sulphides with very high deviations from stoichiometry. In the second example, metal-excess chromium sesquisulphide, $Cr_{2+y}S_3$, with moderate nonstoichiometry, will be discussed. The third limiting case concerns few sulphides with a very narrow homogeneity range. It will be represented by metal-deficient manganous sulphide, $Mn_{1-y}S$.

As can be seen, the discussion will be restricted to sulphides with predominant cation sublattice disorder, because with only few exceptions this type of point defect prevails in transition metal sulphides [1–3]. However, the theory and experimental procedure may equally well be utilized in evaluation of chemical- and self-diffusion coefficients in sulphides (and oxides) with predominant anion defects.

2. General remarks

If the growth of any compact homogeneous oxide or sulphide scale on a metal is governed by the volume (lattice) diffusion of cations, the parabolic rate constant of the reaction is related to the self-diffusion coefficient of the metal in the compound (Me_mX_n) forming the scale by the familiar Wagner's equation [13]

$$k'_p = (1/2)Z_c/|Z_a| \int_{p^I_{x_2}}^{p^{II}_{x_2}} D_{Me} d\ln p_{x_2} \qquad (1)$$

where Z_c and Z_a denote cation and anion valencies, respectively (Me^{Z_c+} and X^{Z_a-}) and k'_p is the parabolic rate constant ($cm^2 s^{-1}$) according to Tammann's parabolic rate law

$$dx/dt = k'_p/x \qquad (2)$$

where x is the scale thickness after time t, $p^I_{x_2}$ and $p^{II}_{x_2}$ denote oxidant pressure (activity) at the metal/scale and scale/gas interfaces, respectively.

From Equation 1 it follows that if the self-diffusion coefficient of cations in a compound forming the scale is known as a function of oxidant activity, the parabolic rate constant of the reaction can be calculated and compared with that determined experimentally. The quantitative agreement of both these values may be considered as a direct proof that under given experimental conditions grain-boundary and dislocation-pipe diffusion virtually does not contribute to the overall matter transport through the scale. When, on the other hand, the calculated k'_p value is lower than that obtained experimentally, it strongly suggests that the mechanism of scale growth is more complex and cannot be described in terms of Wagner's theory of metal oxidation, assuming only volume diffusion through point defects.

This procedure has frequently been used in studying the mechanism of metal oxidation, because a number of self-diffusion data in oxides are available in the literature. By contrast, very scant information is so far available on self-diffusion rates in metal sulphides. As already mentioned, the only well-documented exception constitutes non-stoichiometric ferrous sulphide, $Fe_{1-y}S$. Predominant point defects in this compound are cation vacancies, as a result of which $D_{Fe} \gg D_S$, and the sulphide scale on iron is growing by the outward volume diffusion of cations. An analogous type of disorder is observed in many other transition metal sulphides. However, transport properties of these compounds remain unclear.

From the theory of diffusion in solids it follows that the self-diffusion coefficient of cations in a given nonstoichiometric compound ($Me_{1-y}X$ or $Me_{1+y}X$) may readily be calculated from chemical diffusion data if the deviation from stoichiometry and thereby the defect concentration is known as a function of oxidant activity [14, 15]. In contrast with self-diffusion data, the homogeneity range of many sulphides has been determined with a sufficient accuracy. Thus, chemical diffusion coefficients may be utilized for description of the transport properties of the discussed materials.

3. Chemical diffusion

Chemical diffusion is the process of migration of defects under their concentration gradient [14, 15]. The chemical diffusion coefficient, $\tilde{D}$, is then a direct measure of the rate of defect migration in a given solid under non-equilibrium conditions. In the case of nonstoichiometric sulphides or oxides, the chemical diffusion coefficient can be obtained from thermogravimetric measurements of mass changes of a given sample as a function of time when going from one thermodynamic equilibrium state to another. If a metal-deficient $Me_{1-y}X$-type compound is equilibrated at a given temperature and oxidant (X) pressure, the nonstoichiometry, y, reaches a constant value and the mass of the sample remains constant. When the oxidant pressure is suddenly changed to a lower value the sample gradually begins to lose weight as a result of the evolution of gaseous oxidant to the environment, and liberated electrons and cations fill electron holes and cation vacancies, respectively. The concentration of point defects and thereby the nonstoichiometry of the compound decreases, until a new equilibrium is reached. Such a process is called reduction. When, on the other hand, the oxidant pressure is raised to a higher value, the oxidant is bonded on the sample surface, with electrons and cations diffusing there from the lattice, leaving behind electron holes and cation vacancies, respectively. Thus, the weight of the sample, and thereby the concentration of point defects in the compound, increases. In this case, the oxidation process takes place and the nonstoichiometry of the compound increases.

An opposite situation is observed in the case of metal-excess $Me_{1+y}X$-type compounds. That is, if the oxidant pressure is lowered in a given experiment and thereby by the reduction process takes place, the nonstoichiometry of the compound increases because liberated cations and electrons enter interstitial positions. On the other hand, when the oxidation process occurs, cations and electrons diffuse from interstitial positions to the sample surface and the nonstoichiometry of the compound decreases.

This type of reasoning may equally well be applied to non-stoichiometric compounds with predominant anion defects. In this case, however, during the reduction of oxidant-excess MeX_{1+y}-type compounds, the non-stoichiometry, and thereby the defect concentration, decreases as in the case of metal-deficient $Me_{1-y}X$ compounds. The oxidation process, on the other hand, results in the increase in non-stoichiometry. Finally, reduction and oxidation of oxidant-deficient MeX_{1-y} type compounds result in an increase and a decrease in non-stoichiometry, respectively, as in the case of $M_{1+y}X$ compounds.

At high temperatures, chemical reactions at the solid/gas interface proceed usually much faster than the solid-state diffusion because of the higher activation energy of the chemical process than that of diffusion. Thus, the overall reduction and oxidation rates of a given non-stoichiometric compound should be diffusion-controlled, and from the re-equilibration kinetics, the chemical diffusion coefficient may be obtained. The most important point in this experimental procedure is to verify the fundamental assumption concerning the rate-determining step of the overall re-equilibration process. There are two such possibilities. The first one consists in repeating the oxidation and reduction runs under the same experimental conditions. If no hysteresis is observed and the same value of chemical diffusion coefficient is obtained from both re-equilibration runs, it may be considered as experimental proof that the slowest step is the diffusion of defects.

Before discussing the second possibility, the problem of chemical diffusion (migration of defects) in a flat rectangular sample should be considered in terms of Fick's second law.

Fig. 1 shows schematically defect distribution as a function of re-equilibration time, t, in the cross-section of a flat $Me_{1-y}X$-type specimen of thickness $2a$. Predominant defects in this case have been assumed to be doubly ionized cation vacancies and electron holes, the formation of which is described by Reaction (i) on this diagram. (Kröger–Vink notation of defects is used throughout this paper [16].) Dotted lines in this figure mark point-defect (cation vacancy) concentrations at a constant temperature and two different equilibrium states, corresponding to different oxidant pressures: $p^{I}_{X_2}$ and $p^{II}_{X_2}$. In the oxidation experiment (Fig. 1a) the sample is first equilibrated at low oxidant pressure, $p^{I}_{X_2}$, until the defect concentration and non-stoichiometry throughout the cross-section of the specimen reach a corresponding low value, $C^{I}_{V_{Me}}$. When the oxidant pressure is suddenly raised to a higher value, $p^{II}_{X_2}$, the system will gradually approach a new equilibrium state with a higher defect concentration, $C^{II}_{V_{Me}}$. However, the incorporation of oxidant atoms into the sample surface (chemical reaction) proceeds several orders of magnitude faster than the solid-state diffusion. Thus, the concentration of defects in the surface layer of the specimen virtually immediately reaches the higher value, $C^{II}_{V_{Me}}$, corresponding to the new equilibrium. Subsequently, as a result of the concentration gradient, cation vacancies (still being created at the sample surface) diffuse inwards and

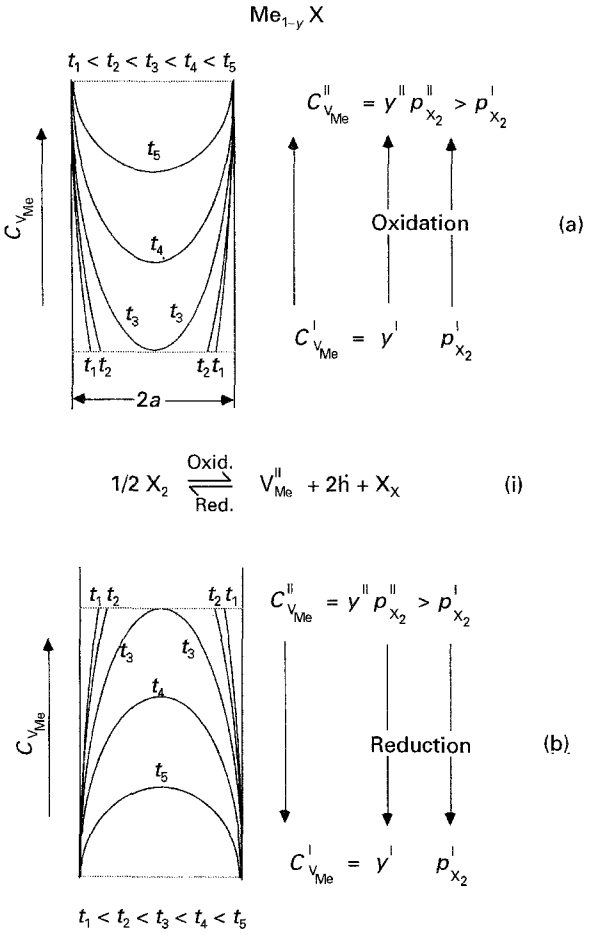

Figure 1 Defect distribution (schematic) in the cross-section of an $Me_{1-y}X$-type specimen as a function of re-equilibration time.

their concentration increases in the deeper and deeper parts of the specimen, until a new equilibrium is established. However, in the early stages of re-equilibration, the defect concentration changes only in the outer parts of the sample and its interior remains unchanged (Fig. 1a, $t < t_3$). In the later stage, on the other hand, the concentration of defects changes over the whole cross-section of the specimen (Fig. 1a, $t > t_3$). Thus, in interpretation of re-equilibration kinetic results, two different solutions of Fick's second law may be applied [17].

For short reaction times ($t < t_3$) the sample can be treated as a semi-infinitive system, where $\tilde{D}t/a^2 < 0.25$, and the appropriate solution is

$$(\Delta m_t/\Delta m_\infty)^2 = 4\tilde{D}t/\pi a^2 \quad (3)$$

where Δm_t is the weight change of the sample after time t, and Δm_∞ is the total weight change of the specimen when the new equilibrium is established.

For the final case, i.e. long re-equilibration times, where $\tilde{D}t/a^2 > 0.15$, the following relationship is obtained

$$[1 - (\Delta m_t/\Delta m_\infty)] = (8/\pi^2)\exp(-\tilde{D}\pi^2 t/4a^2) \quad (4)$$

From these two limiting solutions it follows that for short times the re-equilibration kinetics should be parabolic and in later stages the logarithmic behaviour should be observed

$$\ln[1 - (\Delta m_t/\Delta m_\infty)] = \text{const} - (\tilde{D}\pi^2 t/4a^2) \quad (5)$$

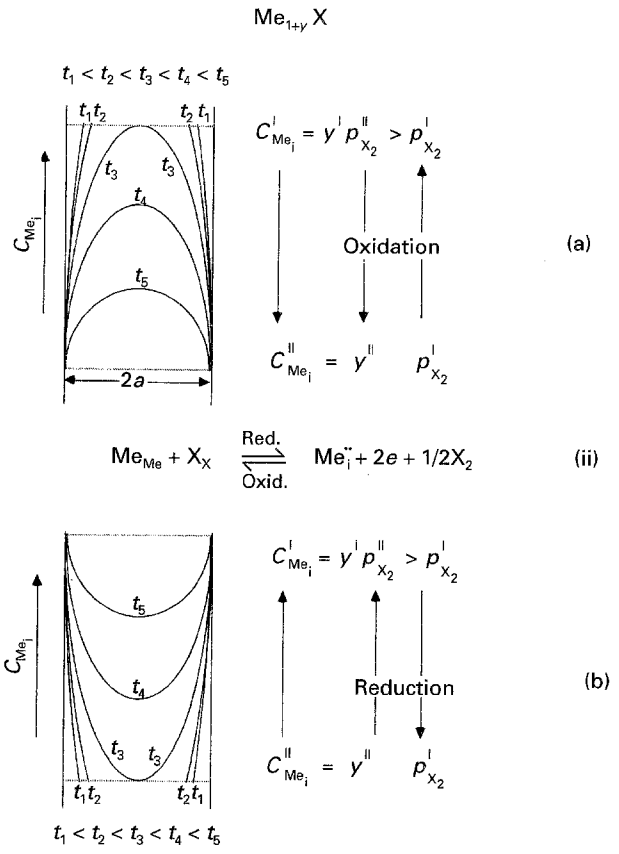

Figure 2 Defect distribution (schematic) in the cross-section of an $Me_{1+y}X$-type specimen as a function of re-equilibration time.

Thus, straight lines should be obtained in parabolic and semi-logarithmic plots, from the slopes of which the same value of chemical diffusion coefficient must be obtained. As can be seen, such an approach offers the second possibility to verify the main assumption of the discussed method.

It should be noted that Equations 3–5 are equally valid for oxidation and reduction runs, because the boundary conditions in the solutions of Fick's second law are identical for both cases. This symmetry follows directly from the comparison of schematic diagrams presented in Fig. 1. The only difference results from the fact that during the oxidation process cation vacancies are being created at the sample surface and diffuse inwards, while during the reduction, the concentration gradient of defects is opposite, because the defects are annihilated at the sample surface and diffuse there from the interior of the lattice (Fig. 1b).

An analogous situation is observed in the case of metal excess $Me_{1+y}X$-type compounds, as illustrated in Fig. 2. However, in this case during oxidation the concentration of defects decreases, while as a result of reduction it increases (Reaction (ii)) and consequently, defect concentration gradients are opposite to those observed in the case of re-equilibration of $Me_{1-y}X$-type compounds.

4. Defect mobility and self-diffusion coefficient

Before a short discussion of selected experimental results, the correlations between chemical, self- and defect-diffusion coefficients should be mentioned. Chemical diffusion is an ambipolar process of the migration of point defects under their concentration gradient [1, 14, 18, 19]. The mobility of defects, in turn (the direct measure of which is the defect diffusion coefficient) characterizes the rate of random walk of defects in thermodynamic equilibrium. The defect diffusion coefficient, D_d, cannot be determined experimentally, but it can readily be calculated if the chemical diffusion coefficient and defect concentration for a given non-stoichiometric compound are known as a function of oxidant activity. These three important quantities ($\tilde{D}$, D_d and C_d) are interrelated by the following equation

$$D_d = 2\tilde{D}(\mathrm{dln}C_d/\mathrm{dln}p_{x_2}) \quad (6)$$

where C_d and p_{x_2} denote defect concentration expressed in mole fraction (site fraction), and oxidant pressure, respectively. The self-diffusion coefficient of ions, in turn, is given by

$$C_i D_i = C_d D_d \quad (7)$$

where C_i denotes the mole fraction of ions in the sublattice predominantly disordered, and D_i the self diffusion coefficient of ions in this sublattice. Introducing this relation into Equation 6, one obtains the following relationship between self- and chemical diffusion coefficients

$$D_i = 2(C_d/C_i)\tilde{D}(\mathrm{dln}C_d/\mathrm{dln}p_{x_2}) \quad (8)$$

From these short remarks it follows clearly that from chemical diffusion data the self-diffusion coefficient of cations (or anions) may easily be obtained as a function of temperature and oxidant activity if only deviations from stoichiometry of a given compound are known. In addition, these data can also be utilized for calculations of the defect diffusion coefficient (Equation 6), being the direct measure of the defect mobility. Thus, not only the absolute values of self- and defect-diffusion coefficients may be obtained but also the activation entropy and enthalpy of defect diffusion can be calculated. In order to illustrate such a procedure of evaluation of transport properties of sulphides, three examples will be shortly discussed.

4.1. Metal-deficient cobaltous sulphide

Cobalt monosulphide crystallizes in the hexagonal NiAs structure and exists over a large homogeneity range (Fig. 3) as a result of the formation of cation vacancies [20, 21]. The anion sublattice, on the other hand, is considered to be virtually ordered. Thus, the non-stoichiometry, y, in $Co_{1-y}S$ is a direct measure of point-defect concentration. This sulphide is a metallic conductor with little change in electrical conductivity with varying composition. From Fig. 3 it follows that $Co_{1-y}S$ is stable above 747 K and its maximum deviation from stoichiometry (at about 1100 K) reaches the enormous value of $y = 0.172$ ($Co_{0.828}S$). Because of such a high concentration, strong repulsive interaction between cation vacancies is observed [20, 22], and consequently, their concentration is not a simple

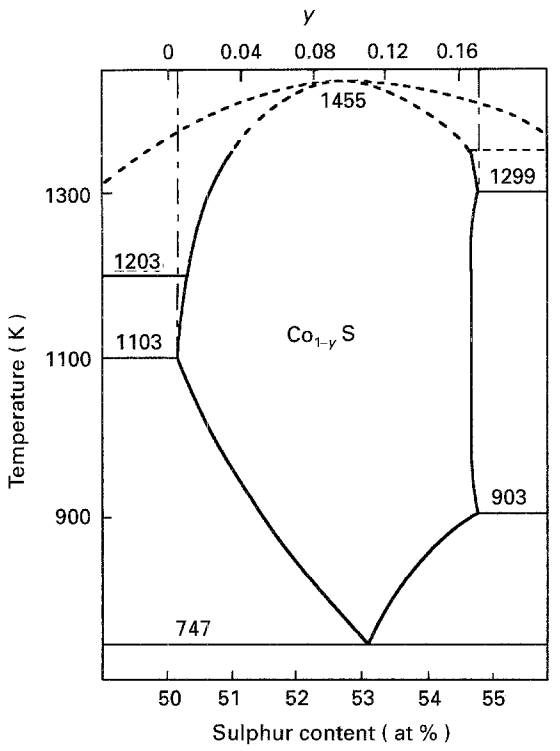

Figure 3 Part of the phase diagram Co–S around the composition of CoS [20] (Reprinted with kind permission from Elsevier Science).

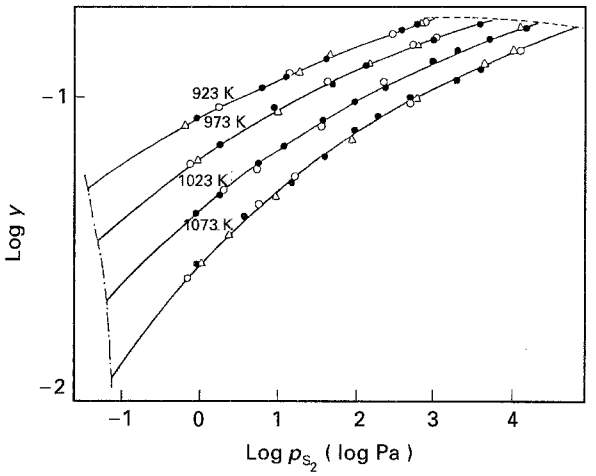

Figure 4 The dependence of non-stoichiometry in $Co_{1-y}S$ on equilibrium sulphur pressure at several temperatures [20, 22]. (——) [20]; (○, ●, △) [22] for samples 1, 2 and 3, respectively; (– · –) phase boundary $Co_9S_8/Co_{1-y}S$; (– – –) phase boundary $Co_{1-y}S/CoS_2$.

power function of sulphur activity (Fig. 4) as in the case of randomly distributed, non-interacting point defects. These data will be used later in calculation of the self-diffusion coefficient of cobalt in $Co_{1-y}S$.

The chemical diffusion coefficient has been studied as a function of temperature (923–1073 K) and sulphur activity (1–10^4 Pa) using the thermogravimetric technique [22]. The apparatus and the details of the experimental procedure have been described elsewhere [22]. In order to determine the possible dependence of the chemical diffusion coefficient on the sulphur activity, the relaxation curves were obtained for small steps in sulphur pressure, traversing the phase field of $Co_{1-y}S$. In every experiment, the sample

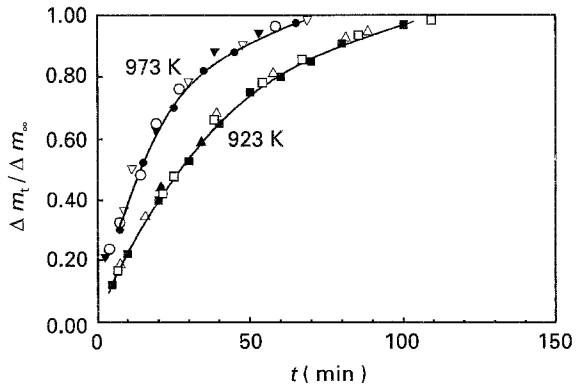

Figure 5 (□, △, ▽, ○) Oxidation and (■, ▲, ▼, ●) reduction relaxation curves for $Co_{1-y}S$ obtained at different temperatures [22]. P_{S_2} intervals: (□, △) 14.0–45.0 Pa, (▽, ○) 2.0–10.0 Pa, (■, ▲) 45.0–14.0 Pa, (▼, ●) 10.0–2.0 Pa.

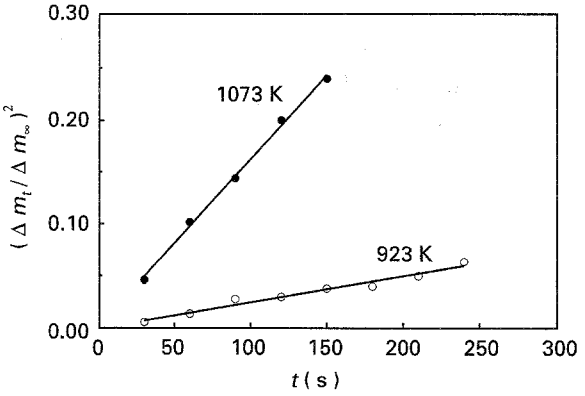

Figure 6 (○) Oxidation and (●) reduction runs for $Co_{1-y}S$ plotted in terms of Equation 3 at different temperatures [22]. P_{S_2} intervals: (●) 1.0–10.0 Pa, (○) 14.0–45.0.

was first equilibrated at a certain partial pressure of sulphur vapour and temperature. A step change in p_{S_2} was then made, and the sample weight was recorded continuously until no further weight change was observed and the sample was again in equilibrium with the new atmosphere. Fig. 5 shows, for illustration, typical re-equilibration curves obtained in two different temperature and pressure intervals. As can be seen, both the oxidation and reduction runs are fully reproducible, the maximum error not exceeding $\pm$ 5%. In addition, no hysteresis was observed between oxidation and reduction runs, clearly indicating that the re-equilibration kinetics of $Co_{1-y}S$ is diffusion controlled. The second important proof of this fundamental assumption results from the fact that the chemical diffusion coefficients calculated from early stages of re-equilibration (Fig. 6) using Equation 3 are virtually identical with those obtained through Equation 5 from long-term experiments (Fig. 7). The results of calculations obtained are summarized in Fig. 8. As can be seen, within the limits of experimental error, $\tilde{D}_{CoS}$ does not depend on sulphide composition (defect concentration). As a consequence, the temperature dependence of this coefficient can be presented by a single straight line in an Arrhenius plot (Fig. 9) and expressed by the following empirical equation [22]

$$\tilde{D}_{CoS} = 0.29\exp[(-110 \pm 8.5\,\mathrm{kJ\,mol^{-1}})/RT] \quad (9)$$

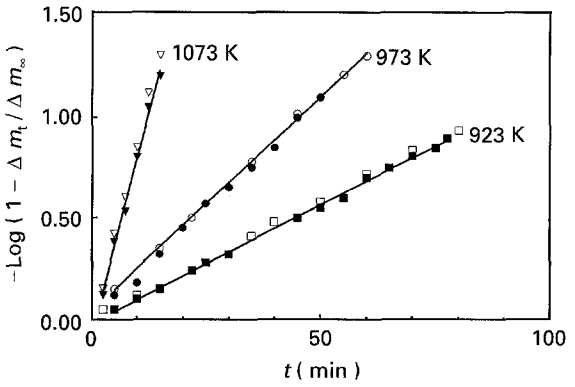

Figure 7 (□, ○, ▽) Oxidation and (■, ●, ▼) reduction runs for $Co_{1-y}S$ plotted in terms of Equation 5 at different temperatures [22]. P_{S_2} intervals: (□) 14.0–45.0 Pa, (○) 140.0–500.0 Pa, (▽) 1.0–10.0 Pa, (■) 45.0–14.0 Pa, (●) 500.0–140.0 Pa, (▼) 10.0–1.0 Pa.

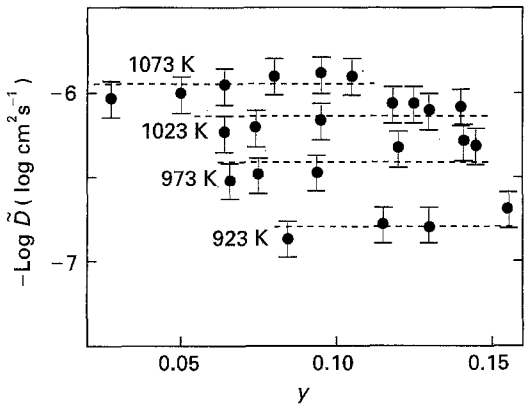

Figure 8 The dependence of the chemical diffusion coefficient in $Co_{1-y}S$ on its composition at several temperatures.

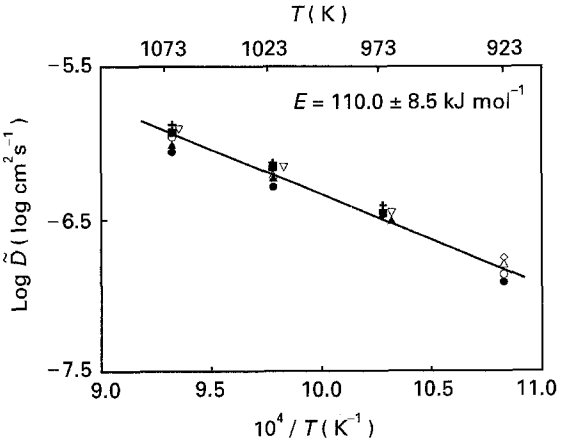

Figure 9 The temperature dependence of the chemical diffusion coefficient in $Co_{1-y}S$ at several sulphur activities [22], P_{S_2} (Pa): (●) 1.0, (▼) 2.0, (■) 4.0, (▲) 10, (△) 14, (○) 45, (+) 100, (◇) 320, (+) 500, (▽) 1000.

These results, together with those of non-stoichiometry presented in Fig. 4, may be used for the calculation of vacancy diffusion coefficient, D_v, and self-diffusion coefficient of cations, D_{Co}, in $Co_{1-y}S$ as a function of temperature and sulphur activity (or sulphide composition).

For the case under discussion, Equation 6 assumes the following form

$$D_v = 2\tilde{D}_{CoS}(d\ln y/d\ln p_{S_2}) \quad (10)$$

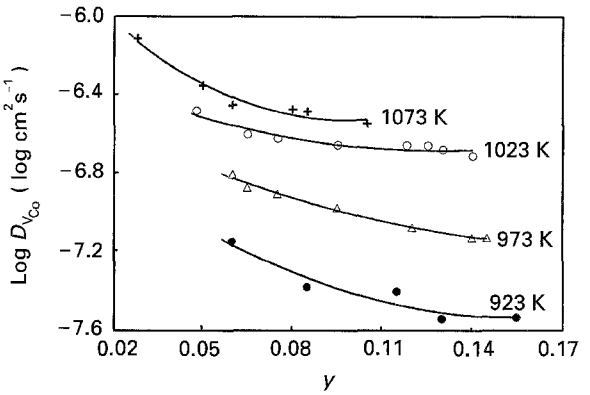

Figure 10 The dependence of the defect-diffusion coefficient in $Co_{1-y}S$ on its composition at several temperatures.

It follows from the above relationship that if the defect concentration is a simple power function of sulphur pressure, the defect-diffusion coefficient should depend on sulphur activity in the same manner as the chemical-diffusion coefficient, i.e. the mobility of point defects in $Co_{1-y}S$ would be independent of their concentration. However, from Fig. 4 it follows that because of repulsive interactions between defects, the non-stoichiometry of cobaltous sulphide is a complex function of sulphur activity. Consequently, the differential in Equation 10 does not assume a constant value at a given temperature, and this must reflect different dependence of $\tilde{D}_{CoS}$ and D_v on sulphide composition. In order to evaluate the dependence of D_v on y, the non-stoichiometry curves shown in Fig. 4 were numerically differentiated, and D_v was calculated as a function of sulphide composition and temperature by means of Equation 10, assuming that the chemical diffusion coefficient is pressure independent. The results of these calculations are shown in Fig. 10. As can be seen, the defect-diffusion coefficient, and thereby the mobility of cation vacancies in $Co_{1-y}S$ decreases as their concentration increases.

As the defect-diffusion coefficient is related to the jump frequency of defects by [15, 18]

$$D_d = \alpha a_0^2 \omega \quad (11)$$

where α is a geometric factor, and a_0 the jump distance traversed by a cation from one vacancy to another, it may be concluded that the jump frequency of cation vacancies in $Co_{1-y}S$ decreases with their increasing concentration. This becomes conceivable if one considers the fact that for such a high lattice disorder, the jump frequency of defects should decrease with their increasing concentration due to the site-blocking effect [23].

The temperature dependence of D_v is shown in Fig. 11 as an Arrhenius plot. As can be seen, the activation energy of vacancy self-diffusion is essentially independent of sulphide composition and thereby can be described by the following empirical equation

$$D_v = D_v^0 \exp[(-135.0 \pm 10.3\ \text{kJ mol}^{-1})/RT] \quad (12)$$

where D_v^0 changes with sulphur activity from 1.25 at $p_{S_2} = 10^3$ Pa up to 1.75 at $p_{S_2} = 10$ Pa.

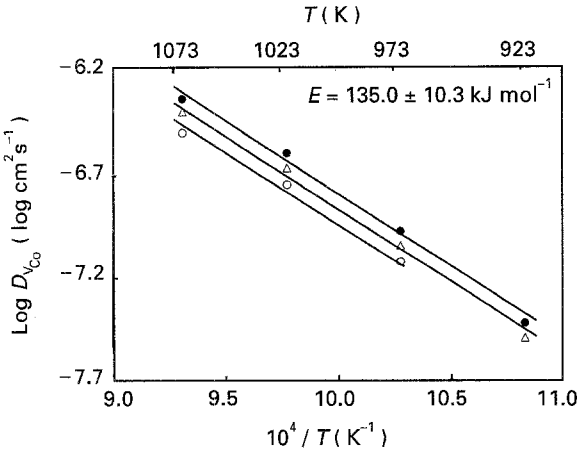

Figure 11 The temperature dependence of the defect-diffusion coefficient in $Co_{1-y}S$ at different sulphur activities, P_{S_2} (Pa): (●) 10, (△) 100, (○) 1000.

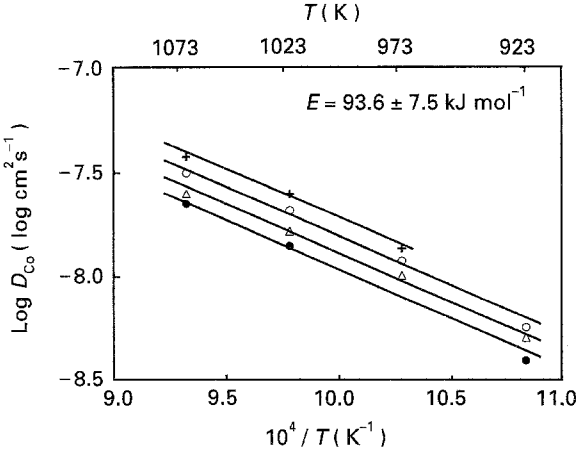

Figure 13 The temperature dependence of the self-diffusion coefficient of cobalt in $Co_{1-y}S$ at different sulphur activities, P_{S_2} (Pa): (●) 1, (△) 10, (○) 100, (+) 1000.

The results described above may be utilized for calculation of the self-diffusion coefficient of cobalt in $Co_{1-y}S$ as a function of temperature and sulphide composition by means of Equation 7 or 8. For the case under discussion, Equation 7 assumes the following form

$$(1 - y)D_{Co} = D_v y \tag{13}$$

Thus

$$D_{Co} = D_v y/(1 - y) \tag{14}$$

Using this relationship, the self-diffusion coefficient of cobalt in the cobaltous sulphide has been calculated as a function of T and p_{S_2}, and the results of these calculations are shown in Figs 12 and 13 as double logarithmic and Arrhenius plots, respectively. As can be seen, the self-diffusion rate of cations in $Co_{1-y}S$ increases very slightly with increasing sulphur activity (Fig. 12), much slower than does the non-stoichiometry (Fig. 4). This is the result of the "compensation effect": decreasing defect mobility (Fig. 10) with simultaneous increase of defect concentration. On the other hand, the activation energy of diffusion is pressure independent (Fig. 13) and consequently, the temperature dependence of the self-diffusion rate of

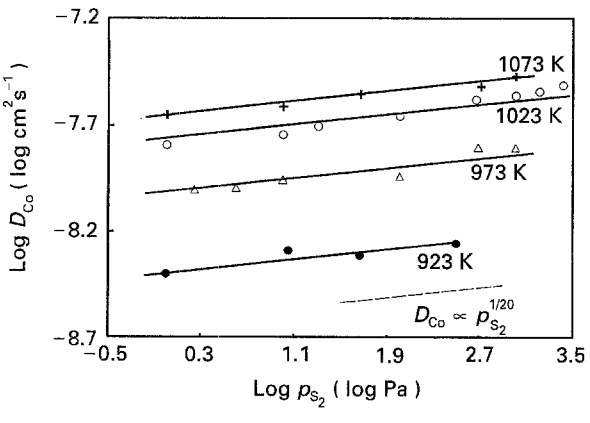

Figure 12 The dependence of self-diffusion coefficient of cobalt in $Co_{1-y}S$ on sulphur pressure at several temperatures [22].

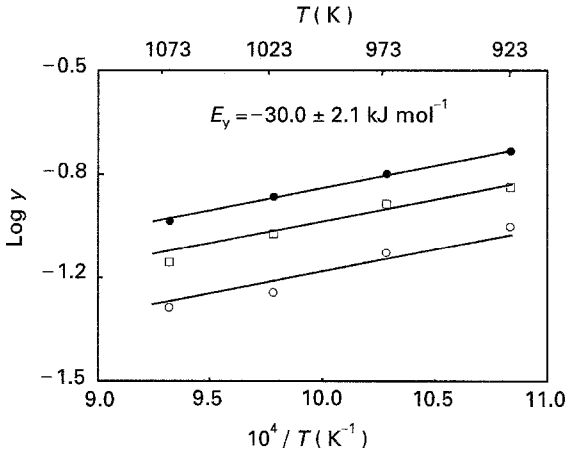

Figure 14 The temperature dependence of non-stoichiometry in $Co_{1-y}S$ at different sulphur activities, P_{S_2} (Pa): (●) 10, (□) 100, (○) 1000.

cations in cobaltous sulphide can be expressed in the following empirical equation

$$D_{Co} = 8.9 \times 10^{-4} p_{S_2}^{1/20} \times \exp[(-93.6 \pm 7.5\ \text{kJ mol}^{-1})/RT] \tag{15}$$

As can be seen, the activation energy of cobalt self-diffusion, $E_D = 93.6\ \text{kJ mol}^{-1}$, is lower than that of the vacancy diffusion in $Co_{1-y}S$, which is equal to $135\ \text{kJ mol}^{-1}$ (Equation 12). This a priori unexpected behaviour results from the fact that due to repulsive interactions of cation vacancies, their concentration in $Co_{1-y}S$ decreases with increasing temperature (Fig. 4) and consequently, the apparent enthalpy of defect formation assumes a negative value (Fig. 14) and equals approximately $-30\ \text{kJ mol}^{-1}$. As the self-diffusion coefficient is given by Equation 7 the activation energy of self-diffusion at a constant oxidant activity is the sum of enthalpies of defect formation and migration in the crystal lattice. Thus, the activation energy of cobalt self-diffusion in $Co_{1-y}S$ must be lower than that of vacancy diffusion by the value equal to the apparent enthalpy of defect formation. The results obtained are in qualitative agreement with these considerations.

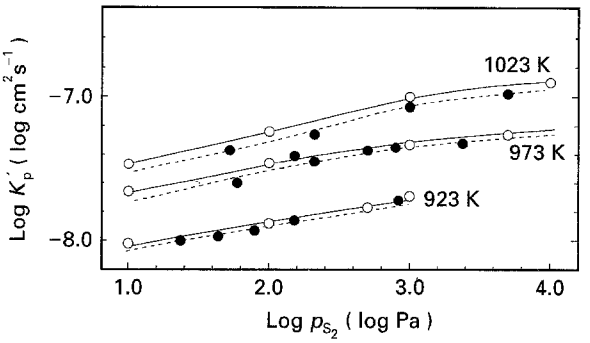

Figure 15 The pressure dependence of the growth rate of $Co_{1-y}S$ scale layer on cobalt at different temperatures. (●) Experimentally determined from the sulphidation kinetics [43], (○) calculated from D_{CoS} and non-stoichiometry, y.

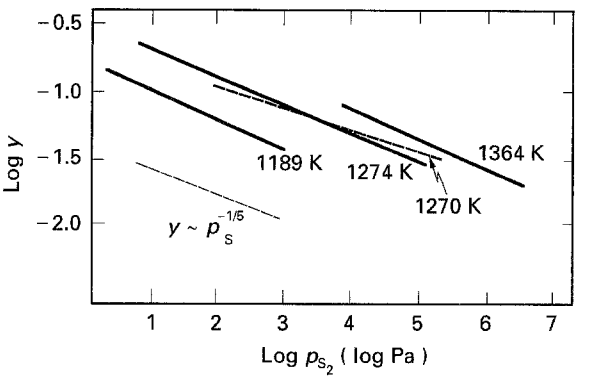

Figure 16 The dependence of non-stoichiometry in $Cr_{2+y}S_3$ on sulphur activity at several temperatures [24, 25]. (——) [24], (– – –) [25].

Summing up these remarks, it seems reasonable to compare the growth rate of the $Co_{1-y}S$ scale layer on cobalt with that calculated from the chemical diffusion coefficient. From Wagner's theory of metal oxidation [13] it follows that in the case under discussion the parabolic rate constant of $Co_{1-y}S$ layer formation is related to $\tilde{D}_{CoS}$ by the following simple equation

$$k_p' = \tilde{D}_{CoS}(C_v^{(a)} - C_v^{(i)}) \tag{16}$$

where k_p' is expressed in cm^2 s^{-1}, according to Equation 1, and $C_v^{(a)}$ and $C_v^{(i)}$ denote cation vacancy concentrations, expressed in mole fraction, at outer and inner phase boundaries of the growing $Co_{1-y}S$ layer, ie. at $T > 900$ K and $p_{S_2} < p_{CoS_2}^{(d)}$, at $Co_{1-y}S/S_2$ and $Co_9S_8/Co_{1-y}S$ interfaces, respectively ($p_{CoS_2}^{(d)}$ denotes the dissociation pressure of the CoS_2 phase). This vacancy concentration gradient is equal to the difference in non-stoichiometry across the growing $Co_{1-y}S$ layer

$$C_v^{(a)} - C_v^{(i)} = y^{(a)} - y^{(i)} = \Delta y \tag{17}$$

Equation 16 may then be written in the following form

$$k_p' = \tilde{D}_{CoS}\Delta y \tag{18}$$

Δy values can easily be calculated from the diagram presented in Fig. 4. Using these data and Equation 18, k_p' has been calculated as a function of temperature, T, and sulphur activity, p_{S_2}, ranges where the double-layer ($Co_9S_8/Co_{1-y}S$) scale on cobalt is formed. The results of these calculations are shown in Fig. 15 on the background of experimentally determined rates of $Co_{1-y}S$ formation. The latter k_p' values have been obtained from measurements of the thickness of $Co_{1-y}S$ layer as a function of time of cobalt sulphidation. As can be seen, the agreement between calculated and experimentally determined growth rates of $Co_{1-y}S$ layer is satisfactory, indicating clearly that the rate-determining step of this process is the volume diffusion of cations.

4.2. Metal excess chromium sulphide

Chromium sesquisulphide has been found to be a metal-excess n-type semiconductor with interstitial cations and quasi-free electrons as predominant defects ($Cr_{2+y}S_3$) [24, 25]. Consequently, the non-stoichiometry of this sulphide decreases with increasing sulphur activity, as illustrated in Fig. 16. From this diagram it follows also that this relationship can be described by a simple power function

$$y = \text{const } p_{S_2}^{-1/n} \tag{19}$$

which implies that in spite of rather high concentration, point defects in the discussed sulphide do not interact and are randomly distributed in the crystal lattice. From the slope of straight lines presented in Fig. 16 it may be inferred that above 1000 K interstitial cations in $Cr_{2+y}S_3$ are, in the majority, fully ionized. This conclusion follows simply from the application of mass action law to respective defect equilibria

$$Cr_{Cr} + 1.5S_S \rightleftarrows Cr_i^x + 3/4S_2 \tag{20}$$

$$Cr_{Cr} + 1.5S_S \rightleftarrows Cr_i^{\cdot} + e^- + 3/4S_2 \tag{21}$$

$$Cr_{Cr} + 1.5S_S \rightleftarrows Cr_i^{\cdot\cdot} + 2e^- + 3/4S_2 \tag{22}$$

$$Cr_{Cr} + 1.5S_S \rightleftarrows Cr_i^{\cdot\cdot\cdot} + 3e^- + 3/4S_2 \tag{23}$$

Corresponding equilibrium constants assume the form

$$K_1 = [Cr_i^x]\,p_{S_2}^{3/4} \tag{24}$$

$$K_2 = [Cr_i^{\cdot}]\,[e^-]\,p_{S_2}^{3/4} \tag{25}$$

$$K_3 = [Cr_i^{\cdot\cdot}]\,[e^-]^2\,p_{S_2}^{3/4} \tag{26}$$

$$K_4 = [Cr_i^{\cdot\cdot\cdot}]\,[e^-]^3\,p_{S_2}^{3/4} \tag{27}$$

Application of the appropriate electroneutrality conditions yields

$$[Cr_i^x] = \text{const } p_{S_2}^{-3/4} = \text{const } p_{S_2}^{-1/1.33} \tag{28}$$

$$[Cr_i^{\cdot}] = \text{const } p_{S_2}^{-3/8} = \text{const } p_{S_2}^{-1/1.67} \tag{29}$$

$$[Cr_i^{\cdot\cdot}] = \text{const } p_{S_2}^{-3/12} = \text{const } p_{S_2}^{-1/4} \tag{30}$$

$$[Cr_i^{\cdot\cdot\cdot}] = \text{const } p_{S_2}^{-3/16} = \text{const } p_{S_2}^{-1/5.3} \tag{31}$$

As can be seen, the exponent in Equation 31 representing the pressure dependence of the concentration of completely ionized interstitial cations is only slightly lower than 1/5, while in the case of doubly, singly and non-ionized point defects this exponent equals 1/4, 1/1.67 and 1/1.33, respectively. On the other hand, from Fig. 16 it follows clearly that the experimentally

determined exponent in empirical Equation 19 is close to 1/5. It implies that at high temperatures ($T > 1000$ K) triply ionized interstitial cations constitute the prevailing disorder in chromium sesquisulphide. This conclusion will be utilized later in calculation of the self-diffusion coefficient of chromium in $Cr_{2+y}S_3$ as a function of temperature and sulphur activity.

As in the case of cobaltous sulphide, chemical-diffusion coefficients in $Cr_{2+y}S_3$ have been obtained from re-equilibration kinetics determined thermogravimetrically in the apparatus described elsewhere [26]. A high-purity chromium sample (99.998% Cr) in the form of flat rectangular prism, 0.02 cm thick and of the total surface area of about 3 cm^2, was sulphidized completely under the given experimental conditions to obtain chromium sesquisulphide of a defined composition, manifesting itself by the constant mass of the sample. After the thermodynamic equilibrium had been reached, the sulphur pressure in the reaction chamber was suddenly changed and the re-equilibration kinetics was followed by measuring the mass change of the specimen as a function of time until a new equilibrium was attained. In order to prove the main assumption, concerning the rate-determining step of the overall re-equilibration kinetics, both oxidation and reduction runs have been measured [27].

All re-equilibration experiments have been carried out, as in the case of $Co_{1-y}S$, within the temperature and pressure ranges corresponding to the phase field of $Cr_{2+y}S_3$, i.e. where this sulphide is the only thermodynamically stable compound in the chromium–sulphur system. As chromium sesquisulphide is the highest valence compound in this system, the only restriction in choosing appropriate thermodynamic conditions resulted from the Cr_2S_3/Cr_3S_4 phase boundary. The corresponding part of the chromium–sulphur phase diagram is shown in Fig. 17 [27]. Using these data, suitable pressure intervals were chosen for every applied temperature between 1073 and 1373 K.

Fig. 18 shows, for illustration, oxidation and reduction curves of re-equilibration kinetics obtained at 1273 K. As can be seen, both oxidation and reduction runs were fully reproducible and no hysteresis has

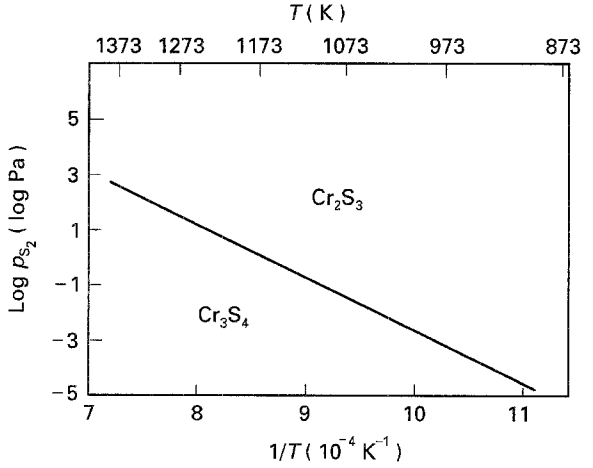

Figure 17 Part of the Cr–S phase diagram [27].

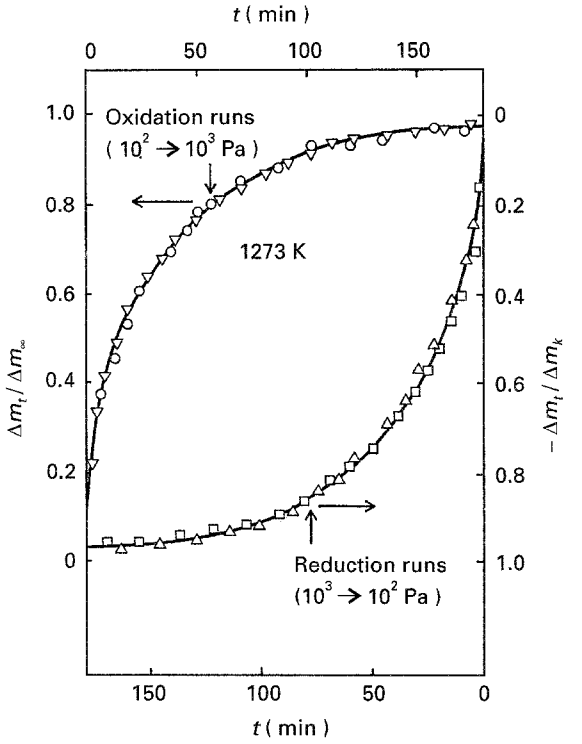

Figure 18 Oxidation and reduction curves for $Cr_{2+y}S_3$ obtained at 1273 K [27].

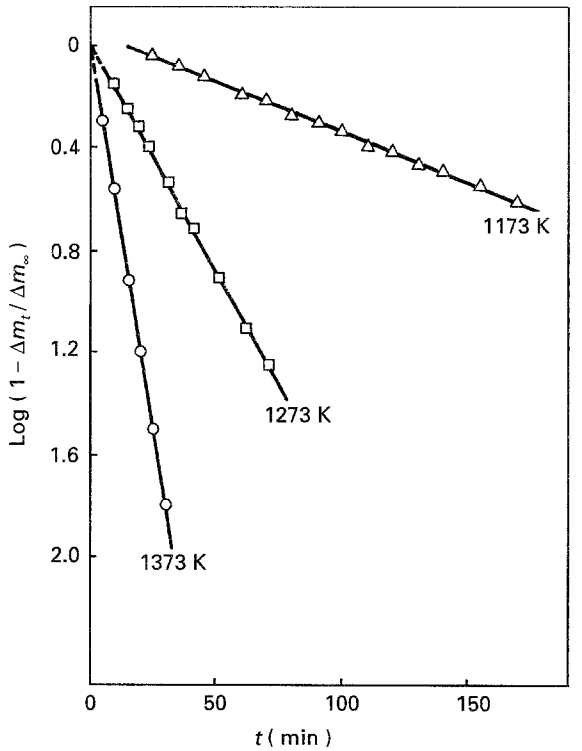

Figure 19 Oxidation and reduction runs for $Cr_{2+y}S_3$ plotted in terms of Equation 5 [27]. (○) 10^4–10^3 Pa, (□) 10^3–10^4 Pa, (△) 10^4–10^2 Pa.

been observed, clearly indicating that the over-all re-equilibration process was diffusion controlled. In agreement with this, straight lines were obtained in semilogarithmic plot for both oxidation and reduction runs (Fig. 19) and from these data the chemical diffusion coefficient has been calculated as a function of temperature and sulphur activity using Equation 5.

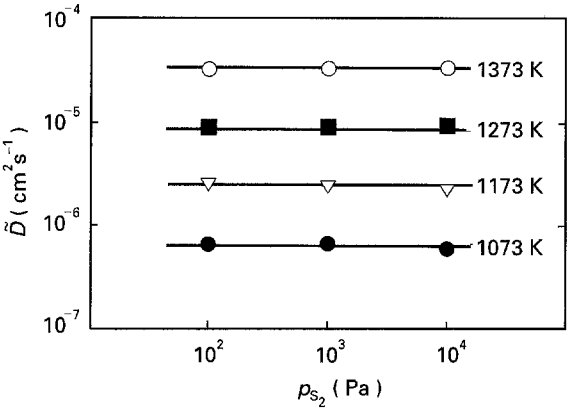

Figure 20 The dependence of the chemical diffusion coefficient in $Cr_{2+y}S_3$ on sulphur activity at several temperatures [27].

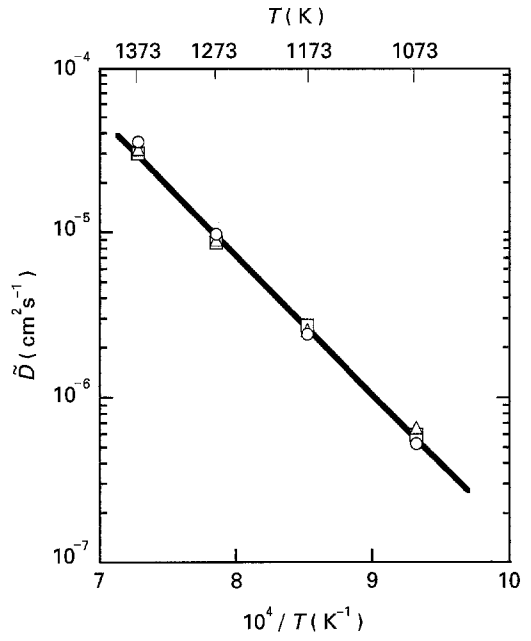

Figure 21 The temperature dependence of the chemical diffusion coefficient in $Cr_{2+y}S_3$ at different sulphur activities [27]; P_{S_2} : (□) 10^2 Pa, (△) 10^3 Pa, (○) 10^4 Pa.

The results of these calculations are shown in Figs. 20 and 21 in double logarithmic and Arrhenius plots, respectively. As can be seen, $\tilde{D}_{Cr_2S_3}$ is pressure independent (Fig. 20) and consequently, the activation energy of chemical diffusion in $Cr_{2+y}S_3$ does not change with sulphide composition (Fig. 21). Thus, the dependence of chemical-diffusion coefficient on temperature may be described by the following empirical equation

$$\tilde{D}_{Cr_2S_3} = 50.86 \exp[(-163.5\ \text{kJ mol}^{-1})/RT] \quad (32)$$

In order to calculate defect- and self-diffusion coefficients from chemical diffusion data, the dependence of defect concentration on the sulphur activity should be known. From Fig. 16 it follows that non-stoichiometry of $Cr_{2+y}S_3$ is a linear function of sulphur pressure in a double logarithmic plot with the slope virtually independent of temperature. Thus, the dependence of non-stoichiometry on sulphur pressure and temperature can be approximated by the following empirical relationship

$$y = 1.25 \times 10^2\, p_{S_2}^{-1/4.8} \exp[(-89.9\ \text{kJ mol}^{-1})/RT] \quad (33)$$

In order to obtain the defect concentration as a function of sulphur pressure and temperature this equation should be rearranged, because in the case of chromium sesquisulphide the deviation from stoichiometry is not the direct measure of defect concentration expressed in mole fraction. The relation between these two quantities is given by

$$[Cr_i^{\alpha+}] = y/(2+y) \quad (34)$$

Consequently, the concentration of interstitial cations in $Cr_{2+y}S_3$, as dependent on equilibrium sulphur pressure and temperature, is given by

$$[Cr_i^{\alpha+}] = 62.50\, p_{S_2}^{-1/4.8} \exp[(-89.9\ \text{kJ mol}^{-1})/RT] \quad (35)$$

The exponent 1/4.8 in this equation is equal to the differential in Equation 6 relating the defect and chemical diffusion coefficients. This relationship can then be reduced to the following empirical form

$$D_i = 0.417\, \tilde{D}_{Cr_2S_3} \quad (36)$$

where D_i denotes the diffusion coefficient of interstitial cations in $Cr_{2+y}S_3$ (defect-diffusion coefficient). Introducing into this equation the right-hand side of Equation 32 one obtains the empirical relationship for defect diffusion coefficient

$$D_i = 21.21 \exp[(-163.5\ \text{kJ mol}^{-1})/RT] \quad (37)$$

It follows from these calculations that because of simple defect structure, the mobility of interstitial cations in chromium sesquisulphide does not depend on their concentration. In such a simple defect situation the activation entropy, ΔS_m, and enthalpy, ΔH_m, of defect diffusion can be calculated by comparing empirical Equation 37 with theoretical relationship given by [15, 18]

$$D_d = \alpha a_0^2\, \kappa\nu \exp(\Delta S_m/R)\exp(-\Delta H_m/RT) \quad (38)$$

where α is the geometrical factor, κ the transmission coefficient, ν the vibration frequency, and a_0 is the jump distance. From this comparison it follows directly that $\Delta H_m = 163.5\ \text{kJ mol}^{-1}$. Assuming, in turn, α and $\kappa = 1$ and $a_0 = 0.594$ nm [28], as well as calculating the vibration frequency of cations according to the relation [29]

$$\nu = (2/\pi a_0)(\Delta H_m/M)^{1/2} = 1.90 \times 10^{12}\ \text{s}^{-1} \quad (39)$$

(where M is the atomic weight of chromium) one obtains by combining Equations (37) and (38)

$$\Delta S_m = 67.0\ \text{J mol}^{-1}\,\text{K}^{-1}$$

The self-diffusion coefficient of cations in $Cr_{2+y}S_3$ is a product of the defect diffusion coefficient and their concentration (Equation 7). In the case under discussion, Equation 7 assumes the following form

$$(2+y)D_{Cr} = yD_i \quad (40)$$

Considering Equation 34 one obtains

$$D_{Cr} = [Cr_i^{a+}]D_i \quad (41)$$

Introducing into this relationship empirical Equations 35 and 37 yields

$$D_{Cr} = 1.32 \times 10^3 \, p_{S_2}^{-1/4.8} \exp[(-253.4 \text{ kJ mol}^{-1})/RT] \quad (42)$$

In order to elucidate the physical meaning of the activation energy of chromium self-diffusion in the chromium sesquisulphide, the thermodynamics of point defects should be considered. Assuming that under the discussed experimental conditions ($T > 1000$ K) prevailing disorder in the chromium sesquisulphide is described by Equation 23 and eliminating from Equation 27 the equilibrium constant, K_4, gives

$$[Cr_i^{\cdot\cdot\cdot}] = 1/3[e^-] = (1.27)^{1/4} \, p_{S_2}^{-1/5.3} \exp[(1/4)\Delta S_f/R] \times \exp[-(1/4)\Delta H_f/RT] \quad (43)$$

where ΔS_f and ΔH_f denote entropy and enthalpy of defect formation. Introducing this relation and Equation 38 into Equation 41 results in the following theoretical relationship describing the pressure and temperature dependence of the self-diffusion coefficient of chromium in chromium sesquisulphide, assuming that interstitial cations are fully ionized

$$D_{Cr} = (1/27)^{1/4} \alpha a_0^2 \, \kappa\nu \, p_{S_2}^{-1/5.3} \times \exp[\{(1/4)\Delta S_f + \Delta S_m\}/R] \times \exp[-\{(1/4)\Delta H_f + \Delta H_m\}/RT] \quad (44)$$

Comparison of this relationship with empirical Equation 42 indicates that the activation energy of chromium self-diffusion, E_D, *in* $Cr_{2+y}S_3$ is related to the enthalpies of formation and migration of point defects by the following equation

$$E_D = (1/4)\Delta H_f + \Delta H_m = 253.4 \text{ kJ mol}^{-1} \quad (45)$$

Summing up this short discussion on transport properties of chromium sulphide it seems reasonable to compare the results with those obtained for chromium oxide. Because of very low deviations from stoichiometry and extremely slow self-diffusion, the defect structure and diffusion mechanism of chromium in chromium sesquioxide remain unclear ([4] p. 116, [30]). However, the temperature dependence of the self-diffusion coefficient of cations in single-crystalline Cr_2O_3 has been determined [30]

$$D_{Cr(Cr_2O_3)} = 50.1 \exp[-(497.8 \text{ kJ mol}^{-1})/RT] \quad (46)$$

As can be seen, the activation energy for chromium self-diffusion in the oxide is considerably higher than that in the sulphide. However, the rate of this process in the oxide is many orders of magnitude lower, as illustrated in Fig. 22. This dramatic difference results from both much lower defect concentration and unusually lower defect mobility. Greskovich [31] showed that the defect (vacancy) diffusion coefficient in chromium oxide at 1373 K is of the order of 10^{-12} cm^2 s^{-1} which is more than six orders of magnitude lower than those in majority of transition metal oxides. We will come back to this important problem later.

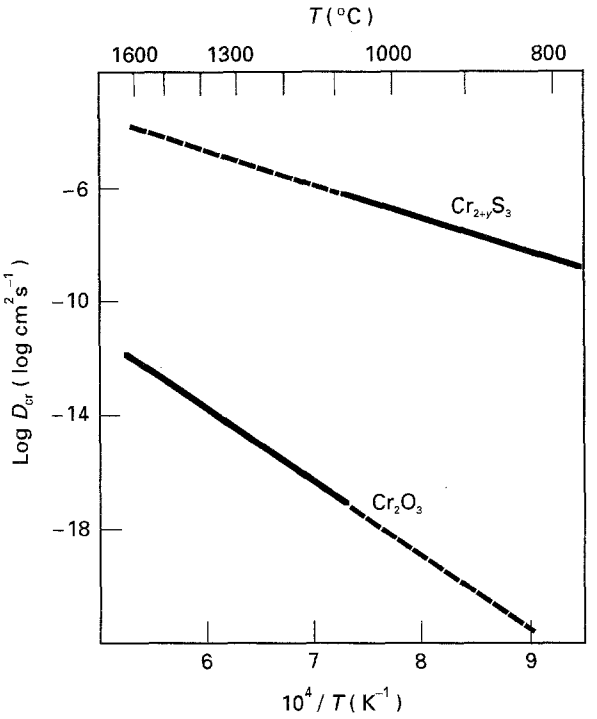

Figure 22 The temperature dependence of the self-diffusion coefficient of cations in chromium oxide [30] and sulphide.

4.3. Metal-deficient manganous sulphide

The high-temperature form of manganous sulphide, α-MnS, is the only stable compound in the Mn–S system above 473 K [32, 33]. Physico-chemical properties of this sulphide have been extensively studied by different authors with various experimental techniques. It has been shown that this compound is a metal-deficient, p-type semiconductor, $Mn_{1-y}S$, with the predominant defects being doubly ionized cation vacancies and electron holes [34, 35]. At very low sulphur activities only, near and at the Mn/MnS phase boundary, this sulphide has been suggested to be a metal-excess n-type semiconductor with interstitial cations and quasi-free electrons as predominant defects [35, 36]. It has been found also that the sulphide scale on manganese grows by the outward diffusion of cations [37]. It may then be assumed that the anion sublattice in $Mn_{1-y}S$ is virtually ordered, the concentrations of anion vacancies and interstitial anions being negligibly small in comparison with cation sublattice disorder.

In contrast with the majority of transition metal sulphides, manganous sulphide shows very low deviations from stoichiometry, and thereby low defect concentration, of the order of that in nickel oxide [1, 34, 35]. This strongly suggests that the interaction between point defects in $Mn_{1-y}S$ should be negligible and their behaviour at high temperatures can be treated in terms of point-defect thermodynamics. Consequently, transport properties of manganous sulphide should also follow the rules of solid-state diffusion theory based on a simple point-defect model [15, 18]. This conclusion is in full agreement with non-stoichiometry data reported by Rau [34]. In very careful and elegant experiments, Rau [34] has been able to determine, with a very high accuracy, deviation

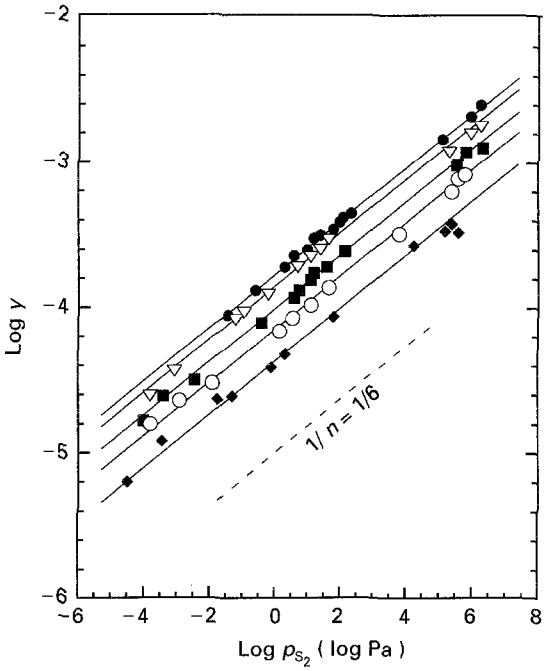

Figure 23 The dependence of non-stoichiometry in $Mn_{1-y}S$ on sulphur activity at several temperatures (replotted from Rau [34]). (●) 1364 K, (▽) 1274 K, (■) 1189 K, (○) 1090 K, (◆) 973 K.

from stoichiometry, y, in $Mn_{1-y}S$ as a function of temperature and sulphur activity over wide T and p_{S_2} ranges. The results of these experiments are summarized in Fig. 23 on a double logarithmic plot. As can be seen, the non-stoichiometry of $Mn_{1-y}S$ is a simple power function of sulphur activity with the slope of 1/6, clearly indicating that cation vacancies in the discussed sulphide do not interact and are fully ionized at $T > 1000$ K. Consequently, the formation of ionic and electronic defects, dominating the disorder over the major part of the phase field of α-MnS, can be described by the following quasi-chemical equation

$$1/2S_2 = V''_{Mn} + 2h^{\cdot} + S_S \qquad (47)$$

Applying to this defect equilibrium the mass action law and the appropriate electroneutrality condition, one obtains the following theoretical dependence of cation vacancy and electron hole concentrations in $Mn_{1-y}S$ on temperature and sulphur activity

$$[V''_{Mn}] = 1/2[h^{\cdot}] = 0.63 p_{S_2}^{1/6} \times \exp[-(1/3)\Delta S_f/R] \times \exp[-(1/3)\Delta H_f/RT] \qquad (48)$$

where ΔS_f and ΔH_f are entropy and enthalpy of defect formation, respectively.

In agreement with this relationship, the experimental results obtained by Rau [34] can analytically be presented by the following empirical equation

$$y = [V''_{Mn}] = 4.77 \times 10^{-2}\, p_{S_2}^{1/6} \times \exp[-(41.5\ \text{kJ mol}^{-1})/RT] \qquad (49)$$

Comparison of Equations 48 and 49 indicates that $\Delta S_f = -64.4\ \text{J mol}^{-1}\,\text{K}^{-1}$ and $\Delta H_f = -124.5$ kJ mol^{-1}.

From this short discussion it follows clearly that the defect structure in metal-deficient manganous sulphide is rather well understood. On the other hand, because of experimental difficulties in studying the diffusion processes in sulphides, direct information is still not available on transport properties of this material. As the non-stoichiometry data were available (Equation 49), the chemical-diffusion coefficient determined as a function of temperature and sulphur activity could successfully be used in calculation of defect mobility and self-diffusion coefficient in $Mn_{1-y}S$.

Unfortunately, in the case of manganous sulphide the application of the thermogravimetric method is problematic. As illustrated in Fig. 23, the maximum deviation from stoichiometry of $Mn_{1-y}S$, even at very high temperatures ($T \approx 1364$ K) is still rather low ($y < 10^{-3}$). Consequently, the determination of the kinetics of mass changes of a given MnS sample in sulphur vapour environments is virtually impossible with sufficient accuracy. However, re-equilibration kinetics of manganous sulphide can successfully be studied using the electrical conductivity method [38, 39]. It has been shown that over the whole p-type homogeneity range of $Mn_{1-y}S$, the concentration of electron holes changes proportionally with the concentration of cation vacancies, and the electrical conductivity, σ, at high temperatures ($T > 900$ K) is the same power function of sulphur activity as non-stoichiometry y

$$\sigma = [h^{\cdot}]\mu_{h^{\cdot}} q_{h^{\cdot}} = \text{const}\ y = \text{const}'\ p_{S_2}^{1/6} \qquad (50)$$

where $\mu_{h^{\cdot}}$ denotes the mobility of electron holes, and $q_{h^{\cdot}}$ their electrical charge. Thus, the mobility of electronic defects can be considered to be independent of their concentration, and the electrical conductivity method may equally well be applied as a thermogravimetric one in determining the chemical diffusion coefficients in the manganous sulphide.

The solutions of Fick's second law are identical to those used in interpretation of thermogravimetric kinetic data. The only difference consists in replacing weight changes of the MnS specimen by those of electrical conductivity. Consequently, for a semi-infinite case, i.e. short re-equilibration times, the solution is

$$(\Delta\sigma_t/\Delta\sigma_\infty)^2 = 4\tilde{D}t/\pi a^2 \qquad (51)$$

and for the finite case, i.e. later stage of re-equilibration

$$[1 - (\Delta\sigma_t/\Delta\sigma_\infty)] = (8/\pi^2)\exp(-\pi^2\tilde{D}t/4a^2) \qquad (52)$$

where $\Delta\sigma_t$ and $\Delta\sigma_\infty$ denote the change of electrical conductivity after time t and the total change of electrical conductivity, respectively.

The starting material for electrical conductivity measurements has been obtained by complete sulphidation of spectrally pure manganese plates (10 mm × 1 mm × 0.1 mm) at 1373 K in pure sulphur vapour at a pressure of 10^3 Pa in the apparatus described elsewhere [26]. The sulphide was then powdered and cold-pressed (1000 kg cm^{-2}) to obtain rectangular specimens (35 mm × 7 mm × 5 mm). These were subsequently annealed for 150 h at 1373 K in sulphur vapour ($p_{S_2} = 10^3$ Pa) in order to obtain the

dense and coarse-grained material. It has been found that after such a treatment the density of α-MnS samples was higher than 98% of the X-ray density, with average grain size of 1 mm.

The electrical conductivity measurements have been performed using the conventional four-probe a.c. method in an apparatus described elsewhere [40]. Both oxidation and reduction kinetics were studied. A new constant sulphur pressure in the reaction chamber was obtained much more rapidly when raising it to higher value (~ 3 min) than lowering it (~ 9 min). Thus, the main part of the experiments was restricted to oxidation runs.

The experiments have been carried out at temperatures ranging from 1073–1373 K and sulphur pressures 10^{-2}–10^{3} Pa. In order to determine the dependence of the chemical diffusion coefficient on defect concentration, the conductivity relaxation curves were obtained for small steps in p_{S_2}, traversing the phase field of $Mn_{1-y}S$. In every experiment the sample was first equilibrated at a certain partial pressure of sulphur vapour and temperature. A step change in p_{S_2} was then created and the electrical conductivity was recorded continuously until no further observable conductivity changes were registered, i.e. the sample was again in equilibrium with the new atmosphere.

Fig. 24 shows typical oxidation curves obtained at 1273 K for two different pressure intervals. As can be seen, the reproducibility of the data was excellent. The analogous results have been obtained at other temperature and pressure intervals. Figs 25 and 26, in turn, illustrate re-equilibration kinetic curves for early stages in the parabolic plot and for later stages in the semilogarithmic system of coordinates, respectively. As can be seen, in agreement with Equations 51 and 52, straight lines have been obtained in both cases, enabling $\tilde{D}_{MnS}$ to be calculated as a function of temperature and sulphur activity. The results of these calculations are shown in Fig. 27.

Two important conclusions can be drawn from those results. Firstly, chemical diffusivities calculated from short- and long-term experiments are virtually the same, clearly indicating that the rate-determining step in the overall re-equilibration process is the solid-state diffusion. Thus, the fundamental assumption of the method is fulfilled, and thereby $\tilde{D}_{MnS}$ values correctly represent the rate of cation vacancy migration in $Mn_{1-y}S$ under non-equilibrium conditions. Secondly, from Fig. 27 it follows that the chemical-diffusion coefficient does not depend on the sulphur activity and thereby on the defect concentration. Thus, the temperature dependence of $\tilde{D}_{MnS}$ constitutes one straight line in the Arrhenius plot (Fig. 28) for all sulphur activities enabling the chemical-diffusion coefficient in $Mn_{1-y}S$ to be expressed by the following empirical equation

$$\tilde{D}_{MnS} = 3.9 \times 10^{-2} \exp[-(76.4 \pm 0.5\ \text{kJ mol}^{-1})/RT] \quad (53)$$

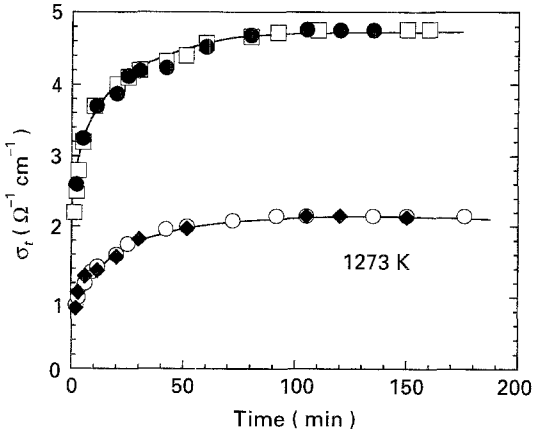

Figure 24 Re-equilibration kinetic curves at two different pressure intervals and four different samples of $Mn_{1-y}S$ [44]. P_{S_2} interval: (●, □) 10^{1}–10^{3} Pa, (◆, ○) 10^{-2}–10^{1} Pa.

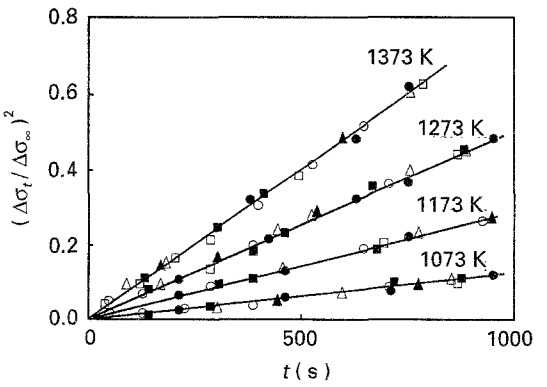

Figure 25 Parabolic plot in the early stage of conductivity change kinetics for $Mn_{1-y}S$ [44]. P_{S_2} intervals: (○, ●) 10^{-2}–10^{3} Pa, (△, ▲) 10^{-2}–10^{1} Pa, (□, ■) 10^{1}–10^{3} Pa.

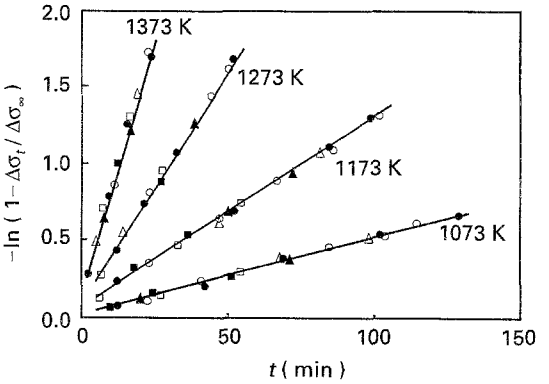

Figure 26 Semi-logarithmic plot in the later stage of conductivity change kinetics for $Mn_{1-y}S$ [44]. P_{S_2} intervals: (○, ●) 10^{-2}–10^{3} Pa, (△, ▲) 10^{-2}–10^{1} Pa, (□, ■) 10^{1}–10^{3} Pa.

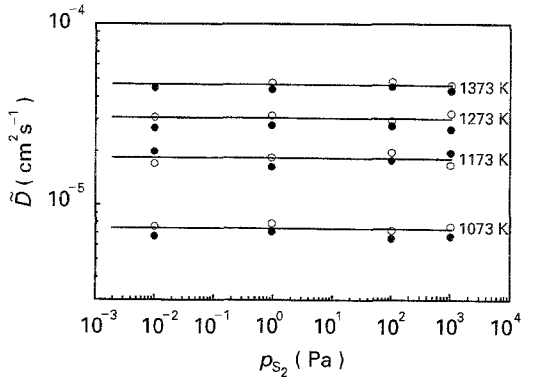

Figure 27 The temperature dependence of the chemical diffusion coefficent in $Mn_{1-y}S$ at several temperatures [44]. (●) Long term, (○) short term.

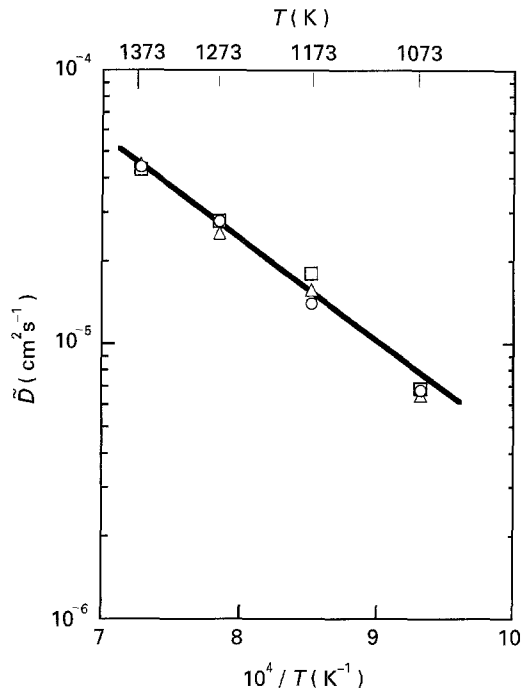

Figure 28 The temperature dependence of the chemical diffusion coefficient in $Mn_{1-y}S$ at several sulphur activities (Arrhenius plot) [44]. P_{S_2} intervals: (□) 10^1–10^3 Pa, (△) 10^{-2}–10^1 Pa, (○) 10^{-2}–10^3 Pa.

In order to calculate the defect (vacancy) diffusion coefficient, Equation 6 should be used in the following form

$$D_v = 2\tilde{D}_{MnS}(d\ln y/d\ln p_{S_2}) \quad (54)$$

From Equation 49 it follows that the differential in Equation 54 is constant and equal to 1/6. Thus, Equation 54 reduces to the following simplified form

$$D_v = 1/3\,\tilde{D}_{MnS} \quad (55)$$

Introducing into this equation the right-hand side of Equation 53 one obtains the empirical relationship describing the vacancy diffusion coefficient in $Mn_{1-y}S$ as a function of temperature

$$D_v = 1.3 \times 10^{-2} \exp[-(76.4 \pm 0.5\ \text{kJ mol}^{-1})/RT] \quad (56)$$

It follows from these calculations that the mobility of cation vacancies in manganous sulphide does not depend on their concentration. This conclusion is not surprising because the concentration of defects in $Mn_{1-y}S$ is very low and they do not interact and are randomly distributed in the crystal lattice.

From the comparison of empirical Equation 56 with theoretical Equation 38 it follows that the activation enthalpy of vacancy diffusion $\Delta H_m = 76.4\ \text{kJ mol}^{-1}$. Assuming, in turn, α and $\kappa = 1$ and $a_0 = 0.530$ nm [32], as well as calculating the vibration frequency of cations according to the relation [29]

$$\nu = (2/\pi a_0)(\Delta H_m/M)^{1/2} = 1.35 \times 10^{12}\ \text{s}^{-1} \quad (57)$$

(where M is the atomic weight of manganese), one obtains by combining Equations 56 and 38 $\Delta S_f = 10.4\ \text{J mol}^{-1}\,\text{K}^{-1}$.

The self-diffusion coefficient of manganese in $Mn_{1-y}S$ can be calculated by means of Equation 7 which for the case under discussion assumes the form

$$(1 - y)D_{Mn} = yD_v \quad (58)$$

As the non-stoichiometry of manganous sulphide is very low ($y < 10^{-3}$) this equation may be approximated to the following form

$$D_{Mn} = yD_{v\cdot} = [V''_{Mn}]D_v \quad (59)$$

Introducing into this relationship the empirical Equations 49 and 56 yields

$$D_{Mn} = 6.2 \times 10^{-4} p_{S_2}^{1/6} \times \exp[-(117.9 \pm 0.7\ \text{kJ mol}^{-1})/RT] \quad (60)$$

On the other hand, by introducing Equations 48 and 38 into Equation 59 one obtains the theoretical relationship describing the temperature and pressure dependences of the self-diffusion coefficient of manganese in $Mn_{1-y}S$

$$D_{Mn} = 0.63\,\alpha a_0^2\,\kappa\nu\,p_{S_2}^{1/6} \times \exp[\{(1/3)\Delta S_f + \Delta S_m\}/R] \times \exp[-\{(1/3)\Delta H_f + \Delta H_m\}/RT] \quad (61)$$

From the comparison of Equations 60 and 61 it follows that the activation energy of manganese self-diffusion, E_D, in manganous sulphide is related to the enthalpies of defect formation and activation of their migration by

$$E_D = (1/3)\Delta H_f + \Delta H_m = 117.9\ \text{kJ mol}^{-1} \quad (62)$$

As the self-diffusion coefficients of manganese in $Mn_{1-y}S$ have been obtained from chemical-diffusion and non-stoichiometry data, it seems reasonable to compare the results of these calculations with other data available in the literature. Unfortunately, because of experimental difficulties, D_{Mn} in $Mn_{1-y}S$ has not been experimentally determined, so far. However, this coefficient has been calculated as a function of temperature and sulphur activity from the kinetics of manganese sulphidation [35, 37, 41]. All these data are shown in Fig. 29 in a double logarithmic plot on the background of the results obtained from $\tilde{D}$ and y in the present paper. It follows clearly from the comparison that the data calculated from manganese sulphidation kinetics are in fairly good agreement with those obtained from chemical-diffusion measurements and deviations from stoichiometry.

During preparation of this paper the first experimentally determined values of D_{Mn} in $Mn_{1-y}S$ were given by Gilewicz–Wolter who performed radiotracer experiments [42]. These few current results have also been marked on the diagram presented in Fig. 29. As can be seen, these experimental data are again in full agreement with those obtained from $\tilde{D}_{MnS}$ and y, as well as from parabolic rate constants of manganese sulphidation. This agreement clearly indicates that at $T > 1000$ K, the sulphide scale on manganese grows by the outward volume diffusion of cations.

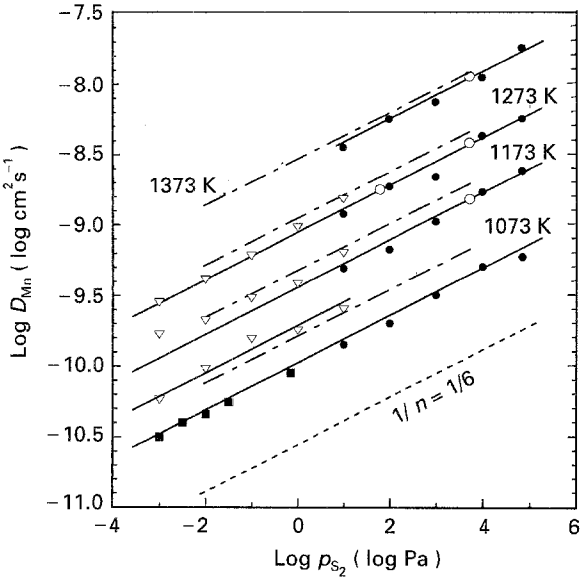

Figure 29 The pressure dependence of the self-diffusion coefficient of manganese in $Mn_{1-y}S$ at several temperatures calculated from $\tilde{D}_{MnS}$ and y, as well as determined experimentally using the radio tracer method [42]. (■), 36, (●) [35], (▽) [41], (○) [42], (---) present work.

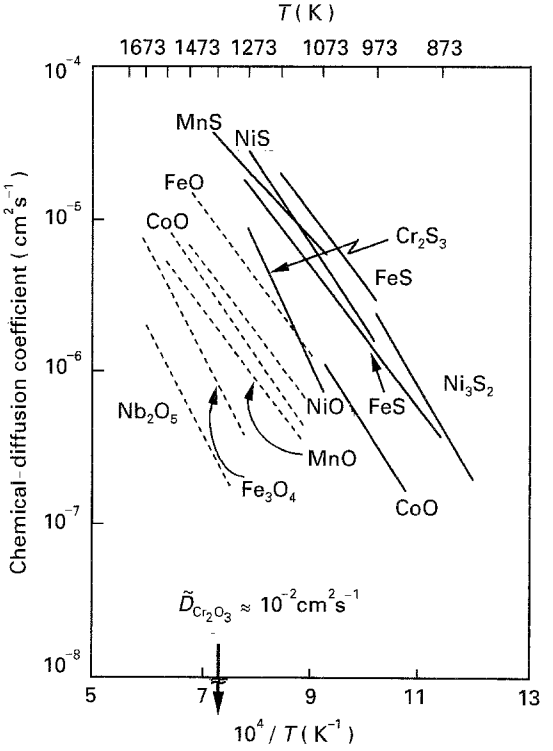

Figure 30 Comparison of the chemical-diffusion coefficient in some metal sulphides and oxides.

5. Conclusions

The results described in the present paper allow the following conclusions to be formulated.

Chemical diffusion coefficients in highly non-stoichiometric sulphides ($Co_{1-y}S$, $Fe_{1-y}S$, $Ni_{1-y}S$) may easily be obtained from re-equilibration kinetic measurements carried out by the thermogravimetric method. When the non-stoichiometry is small and the re-equilibration kinetics difficult or impossible to follow thermogravimetrically, the electrical conductivity method can be applied. However, this method can only be used when the concentration of predominant point defects is strictly proportional to electronic ones (simple defect structure). Such a defect situation is observed, for instance, in metal-deficient manganous sulphide ($Mn_{1-y}S$).

If the non-stoichiometry of a given metal sulphide is known as a function of temperature and sulphur activity, chemical-diffusion data may be utilized to calculate the parabolic rate constants of this metal sulphidation in order to obtain more insight into the growth mechanism of the sulphide scale. Using this procedure it has been shown that as in the case of iron sulphidation, the sulphide scales on cobalt, chromium and manganese grow by the outward, volume diffusion of cations.

Chemical diffusion coefficients may also be utilized for calculation of self-diffusion coefficients of cations (or anions) if the non-stoichiometry data are available. It has been shown that the self-diffusion coefficients of manganese in $Mn_{1-y}S$ obtained in this way are in full agreement with those determined experimentally.

From the comparison of chemical-diffusion coefficients in metal sulphides and oxides it follows (Fig. 30) that, rather surprisingly, the rates of this process, and thereby the mobilities of point defects, do not differ significantly. In fact, the rate of chemical diffusion is generally higher in metal sulphides, but the maximum differences do not exceed one order of magnitude. The only known exception is chromium oxide with about six orders of magnitude lower chemical-diffusion coefficient (Fig. 30). It may then be concluded that in the majority of cases, a significantly higher rate of cation self-diffusion in metal sulphides, in comparison with corresponding oxides, results mainly from the higher defect concentration and not from the greater defect mobility.

Acknowledgement

S. Mrowec thanks Tohoku University for a Visiting Professor position from 1 June 1994 to 31 March 1995.

References

1. S. MROWEC and J. JANOWSKI, in "Selected Topics in High Temperature Chemistry", edited by O. Johannesen and A. G. Andersen (Elsevier, Amsterdam, Oxford, New York, 1989) p. 55.
2. S. MROWEC, *React. Solids* **5** (1988) 241.
3. S. MROWEC and K. PRZYBYLSKI, *High Temp. Mater. Proc.* **6** (1984) 1.
4. P. KOFSTAD, "High Temperature Corrosion" (Elsevier, Amsterdam, 1988) p. 425.
5. V. L. HILL and H. S. MEYER, in "High Temperature Corrosion in Energy Systems", edited by M. R. Rothman (Metallurgical Society of AIME, Warrendale 1985) p. 29.
6. R. H. CONDIT, R. R. HOBBINS and C. E. BIRCHENALL, *Oxid. Met.* **8** (1974) 409.
7. M. DANIELEWSKI, S. MROWEC and A. STOKLOSA, *ibid.* **17** (1982) 77.
8. A. BRUCKMAN and J. ROMAHSKI, *Corr. Sci.* **5** (1965) 185.
9. E. FRYT, W. S. BHIDE and W. W. SMELTZER, *J. Electrochem Soc.* **126** (1979) 684.
10. A. ATKINSON and R. I. TAYLOR, *J. Mater. Sci.* **13** (1978) 427.

11. *Idem, Philos. Mag*, **A39** (1979) 51.
12. *Idem, ibid.* **43** (1981) 979.
13. C. WAGNER, in "Atom Movements" (American Society for Metals, Cleveland, OH, 1951) p. 153.
14. J. B. WAGNER, in "Mass Transport in Oxides" NBS Special Publication 296 (NBS), p. 65.
15. S. MROWEC, "Defects and Diffusion in Solids" (Elsevier, Amsterdam, Oxford, New York, 1980) p. 174.
16. F. KRÖGER, "The Chemistry of Imperfect Crystals" (North-Holland, Amsterdam, 1964).
17. J. CRANK, "The Mathematics of Diffusion" (Oxford University Press, Oxford, 1956).
18. P. KOFSTAD, "Nonstoichiometry, Diffusion and Electrical Conductivity in Binary Metal Oxides" (Wiley-Interscience, New York, London, Sydney, Toronto, 1972) p. 108.
19. H. SCHMALZRIED, "Solid State Reactions" (Academic Press, New York, 1974).
20. H. RAU, *J. Phys. Chem. Solids* **37** (1976) 931.
21. C. N. RAO and K. P. I. PHISHARDY, *Progr. Solid State Chem.* **10** (1978) 207.
22. M. DANIELEWSKI, S. MROWEC and A. WOJTOWICZ, *Oxid. Met.* **35** (1991) 223.
23. G. E. MURCH, "Atomic Diffusion Theory in Highly Defected Solids" (Trans. Tech. S. A., Switzerland, 1980).
24. H. RAU, *J. Less-Common Metals* **55** (1977) 205.
25. M. MIKAMI, K. YAGAKI and N. OHASHI, *J. Phys. Soc. Jpn* **32** (1972) 1217.
26. M. DANIELEWSKI and S. MROWEC, *J. Thermal Anal.* **29** (1984) 1025.
27. M. DANIELEWSKI, J. DABEK, S. MROWEC and G. SIEMINSKA, *Bull. Acad. Polon. Sci. Chem.* **38** (1990) 67.
28. F. JELLINEK, *Acta Crystallogr.* **10** (1957) 620.
29. M. O'KEEFFE and W. I. MOORE, *J. Chem. Phys.* **36** (1962) 3009.
30. A. ATKINSON and R. I. TAYLOR, in "Transport in Non-stoichiometric Compounds", edited by G. Simikovich and S. Shlbican (Plenum Press, New York, 1985) p. 285.
31. C. GRESKQVICH, *J. Am. Ceram. Soc.* **53** (1970) 498.
32. S. FURUSETH, A. KJEKSHUS, *Acta Chem. Scand.* **19** (1965) 1405.
33. J. WAKABAYASHI, H. KOBAYASHI, H. NAGASAKI and S. MINOHARA, *J. Phys. Soc. Jpn* **25** (1968) 227.
34. H. RAU, *J. Phys. Chem. Solids* **39** (1978) 339.
35. M. DANIELEWSKI and S. MROWEC, *Solid State Ionics* **17** (1985) 29.
36. S. MROWEC, M. DANIELEWSKI and H. J. GRABKE, *J. Mater. Sci.* **25** (1990) 537.
37. M. DANIELEWSKI, *Oxid. Met.* **25** (1986) 51.
38. V. CHOWDHRY and R. L. COBLE, *J. Am. Ceram. Soc.* **65** (1982) 336.
39. J. DEREN, Z. JASTRZEBSKI, S. MROWEC and T. WALEC, *Bull. Acad. Polon. Sci. Ser. Sci. Chim.* **19** (1971) 153.
40. S. MROWEC, A. WOJTOWICZ and M. DANIELEWSKI, *Solid State Ionics*, in press.
41. F. A. ELREFAIR and W. W. SMELTZER, *Oxid. Met.* **16** (1981) 267.
42. J. GIKWICZ-WOLTER, *Solid State Commun.*, in press.
43. A. WOJTOWICZ, PhD Thesis, University of Mining and Metallurgy, Cracow, Poland.
44. A. WOJTOWICZ, M. DANIELEWSKI and S. MROWEC, unpublished data.

Received 22 December 1994
and accepted 2 May 1995